



MICROSTRUCTURAL EVALUATION OF PRESELECTED STEELS FOR TURBINE AFTER SUPERCRITICAL CO₂ EXPOSURE

Jan Berka
Lucia Rozumová
Tomáš Melichar
Ladislav Velebil

Supercritical CO₂ cycle

- ❖ The energy conversion cycles with supercritical carbon dioxide (sCO₂)  innovative technology with potential for replacement of conventional steam cycles within various applications such as nuclear, fossil or renewable energy resources
- ❖ Due to extreme operational conditions (temperatures above 550°C and pressures up to 25 MPa)  suitable selection of the materials for the thermal circuit
- ❖ The safety is a critical for the design and operation of the sCO₂ cycle and material selection is one of the most important elements for long-term safe and stable operation of this power system
- ❖ Therefore, this paper aims to investigate the evaluation of pre-selected construction materials, corrosion resistance of four kinds of steels and alloys used in advanced thermal power generation systems in a high-temperature sCO₂ environment.

Experimental system

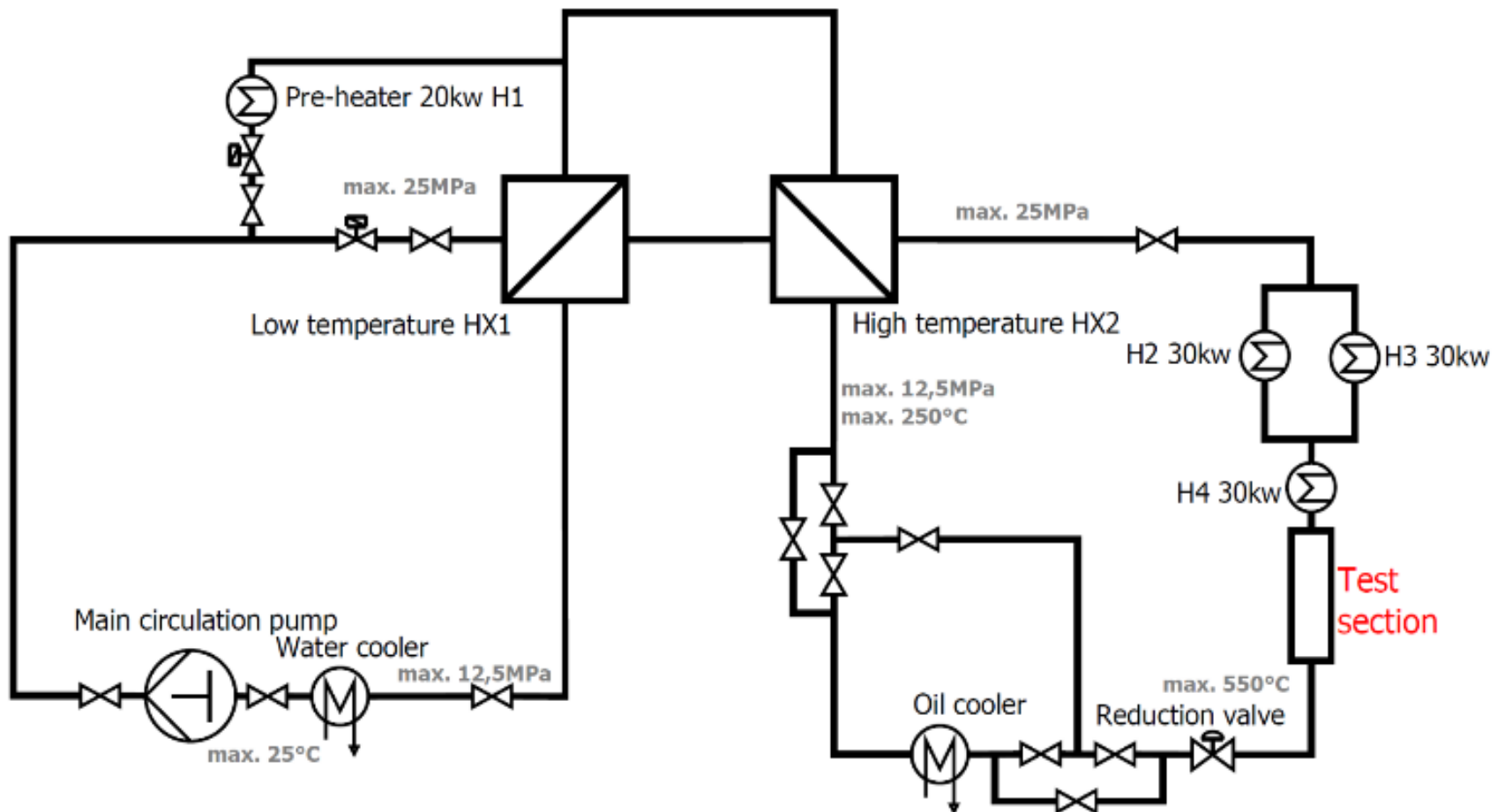
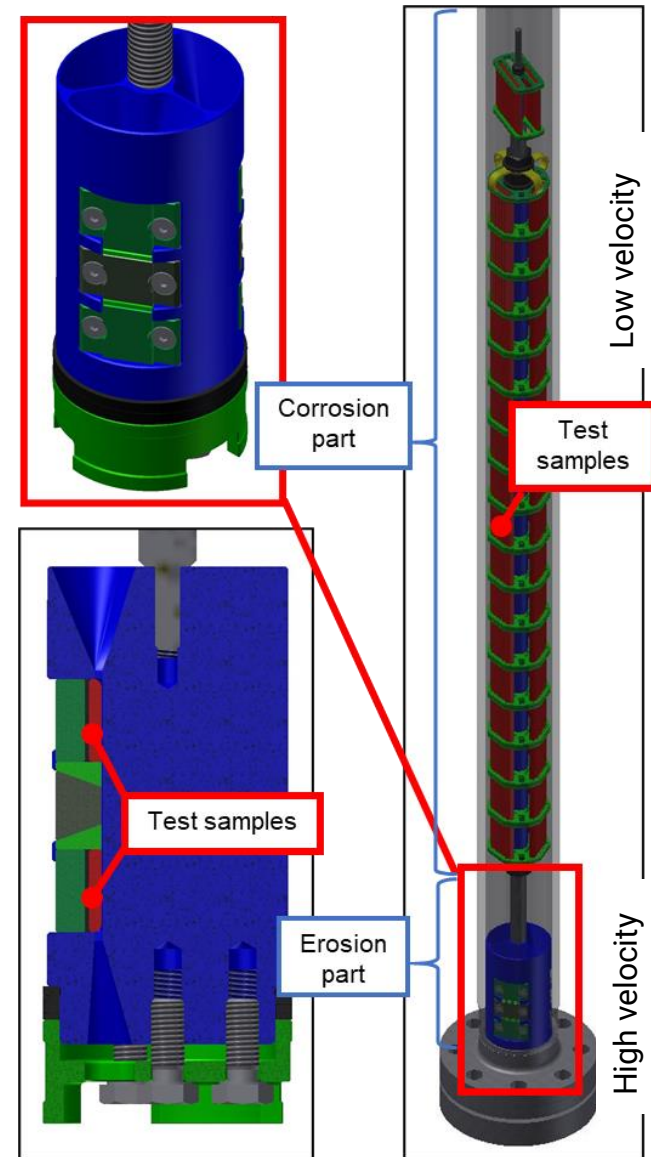


Figure: Simplified diagram of sCO₂ loop

Test section

- ❖ Test section - the parameters of medium were regulated to the demanded values
- ❖ The sample holder - inside the test section
- ❖ The section is made from alloy Inconel 625
- ❖ Holder itself consist of two main body parts: corrosion and erosion part
- ❖ The flow is accelerated by three narrow channels to 100 m.s^{-1} at given parameters 20 MPa, $550 \text{ }^\circ\text{C}$ and mass flow 0.1 kg.m^{-1}
- ❖ The test can be split in two parts based on the sCO_2 flow velocity adjacent to the sample's surfaces:
 1. low velocity ($<10 \text{ m.s}^{-1}$)
 2. high velocity (100 m.s^{-1})



Materials

The experimental materials included four kinds of high-grade heat-resistant alloys:

➔ **FB2** (9-12% Cr steel),

➔ **17-4-PH** (martensitic precipitation-hardening stainless steel),

➔ **625M** (nickel-based superalloy),

➔ **Inconel 718** (corrosion-resistant nickel alloy).

Table: Chemical composition of studied materials (wt.%)

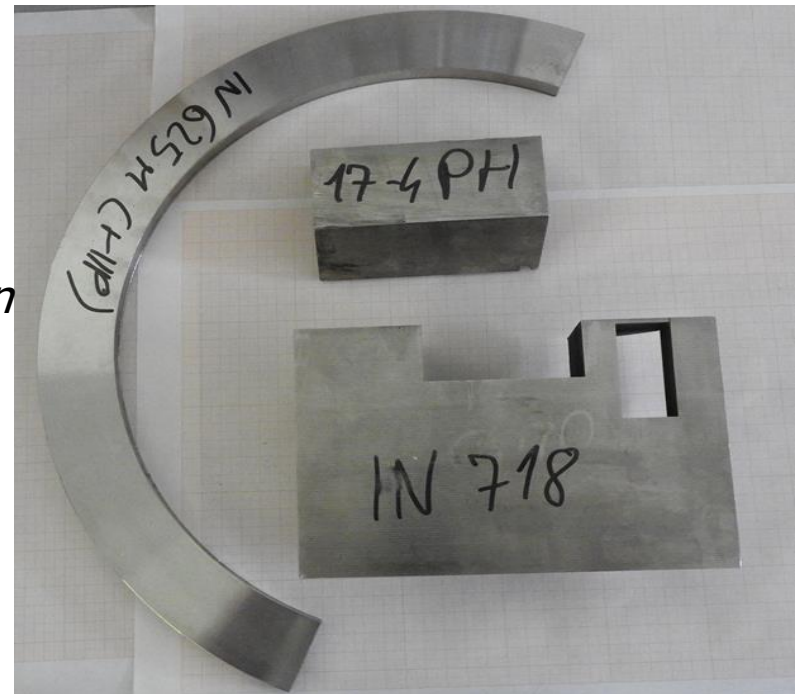
[%]	FB2	17-4-PH	625M	IN718
C	0.13	0.07	0.03	0.08
Mn	0.35	1.0	0.5	0.35
P	-	0.04	0.015	0.015
Cr	9.3	15-17.5	20-23	17-21
Mo	1.50	-	8-10	2.8-3.3
V	0.20	-	-	-
Al	-	-	0.4	0.20-0.80
S	-	0.03	0.015	0.015
Si	-	1	0.15	0.35
Nb	0.05	0.15-0.45	3.15-4.15(Nb+Ta)	4.75-5.5
N	0.020	-	0.2	-
Ni	0.1	3-5	58	50-55
B	0.01	-	-	0.0006
Ti	-	-	0.4	0.65-1.15
Fe	Bal.	Bal.	5	Bal.
Co	1.3	3-5	1	1
Cu	-	-	-	0.3
Ta	-	-	-	0.058

Samples

- ❖ The samples dimensions \longrightarrow 40 mm \times 10 mm \times 2 mm
- ❖ Prior to the test, the samples were ground up to 600 grit SiC paper \longrightarrow then rinsed with deionized water, alcohol, and dried
- ❖ The weight gains were measured before and after the test



Initial material for samples production



Experimental conditions

❖ Temperature  550°C

❖ Pressure  20 Mpa

❖ Flow velocity  $<10 \text{ m}\cdot\text{s}^{-1}$
 $100 \text{ m}\cdot\text{s}^{-1}$

❖ Exposure time  1000 hours

❖ The composition of the sCO_2 atmosphere was 99.995% in the corrosion experiment

Results

Weight gain

- ❖ The table shows the average value of the weight gain, that came from 3 parallel specimens
- ❖ FB2 exhibited the largest weight gain
- ❖ In718 showed the lowest weight gain

Sample	Mass change [%]
FB2	1.17013
17-4-PH	0.00517
625M	0.00675
In718	0.00049

Table: Weight gain of the investigated materials in sCO₂

FB2 sample surface

- ❖ Fig. showed the surface morphology
- ❖ Numerous lumpy structure and pronounced hillock oxides were observed
- ❖ As can we see the Fig. a) before exposure, the oxidation process is very significant in comparison with Fig. b), c), d)

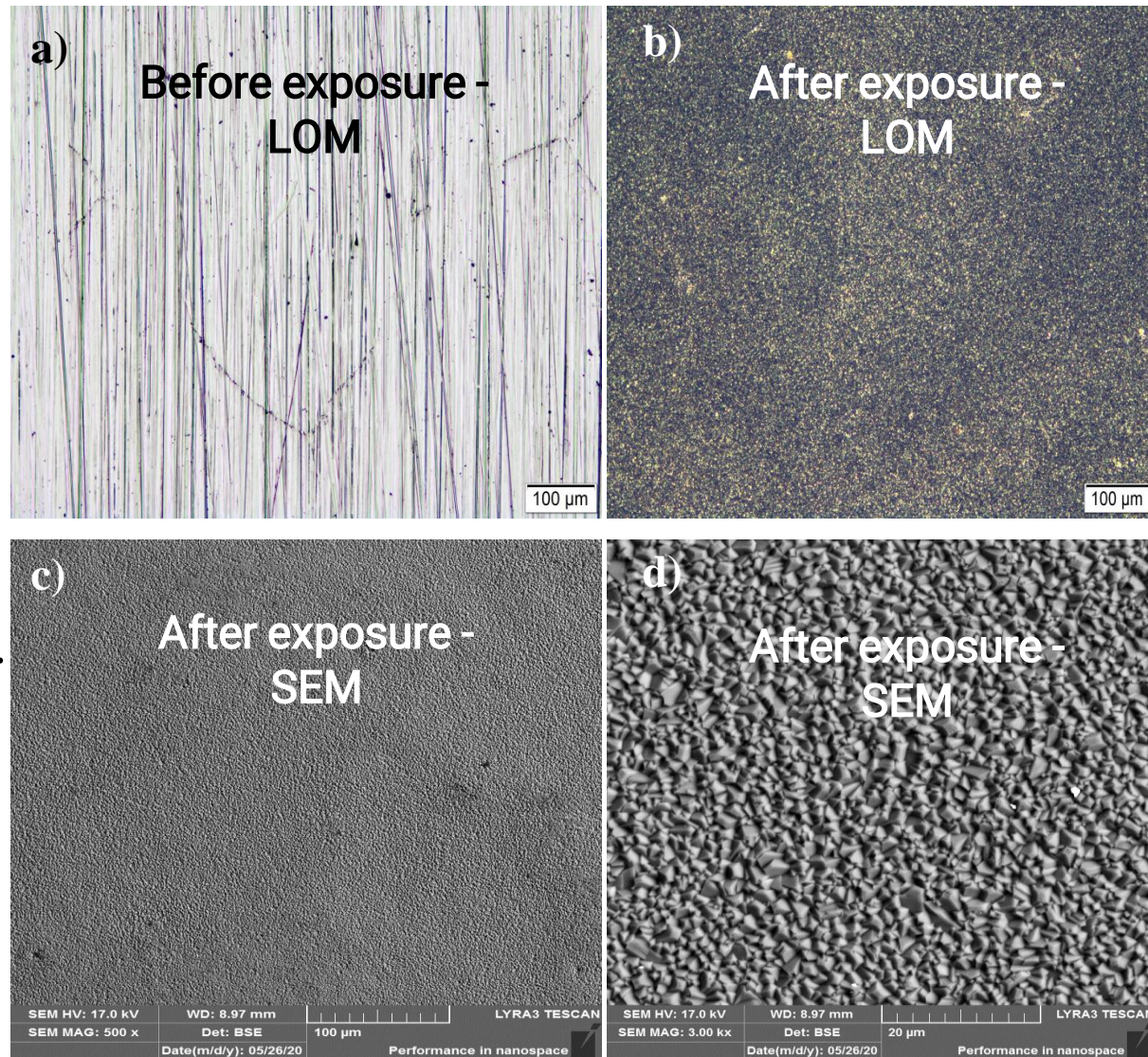


Figure: Surface morphologies of the FB2 before (a) and after sCO₂ exposure (b,c,d)

FB2 sample – cross section

- ❖ Formation of the oxide layer on the Fe-base
- ❖ The oxide layer was thick and homogeneous all over the surface without cracks and defects
- ❖ The oxide layer consists of the inner and outer layer, outer is on the Fe-base and inner is formed from the Fe-Cr-O spinel
- ❖ Under the main layer is internal oxidation zone which is formed from mixed oxide on the Fe-Cr-O base
- ❖ The thickness of these layers is around 22 μm for outer and around 18 μm for inner

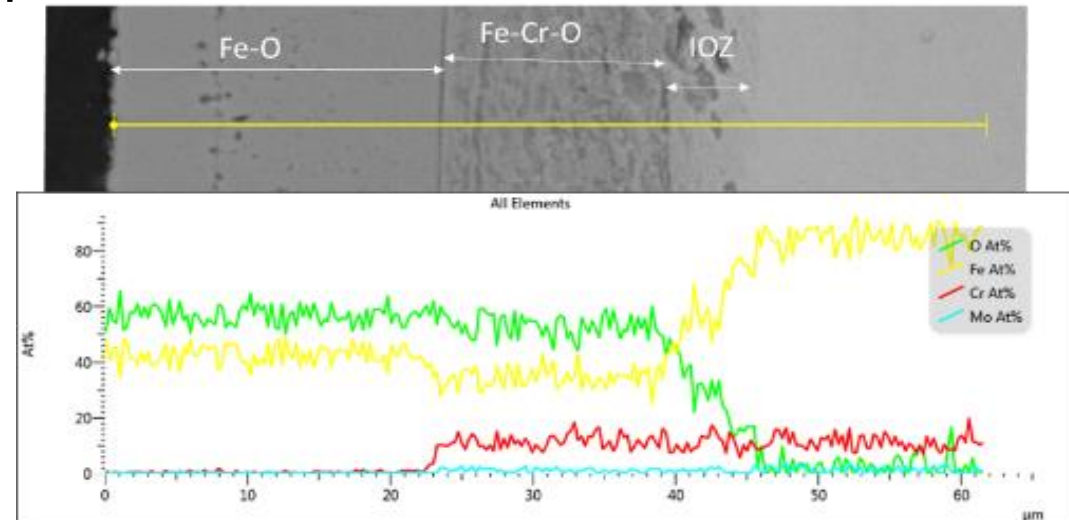
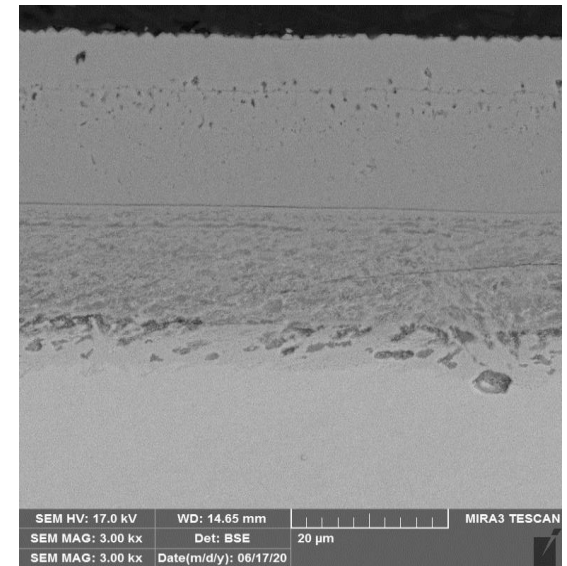


Figure: SEM cross section of the FB2 and EDX linescan of the oxide layer

17-4-PH sample surface

- ❖ Fig. showed the surface morphology
- ❖ The continuous, thin oxide was observed on Fig. b), c), d)
- ❖ The oxide formed on the surface doesn't copy the grooves after mechanical surface treatment
- ❖ Structure of this oxide is very similar like FB2, but thinner

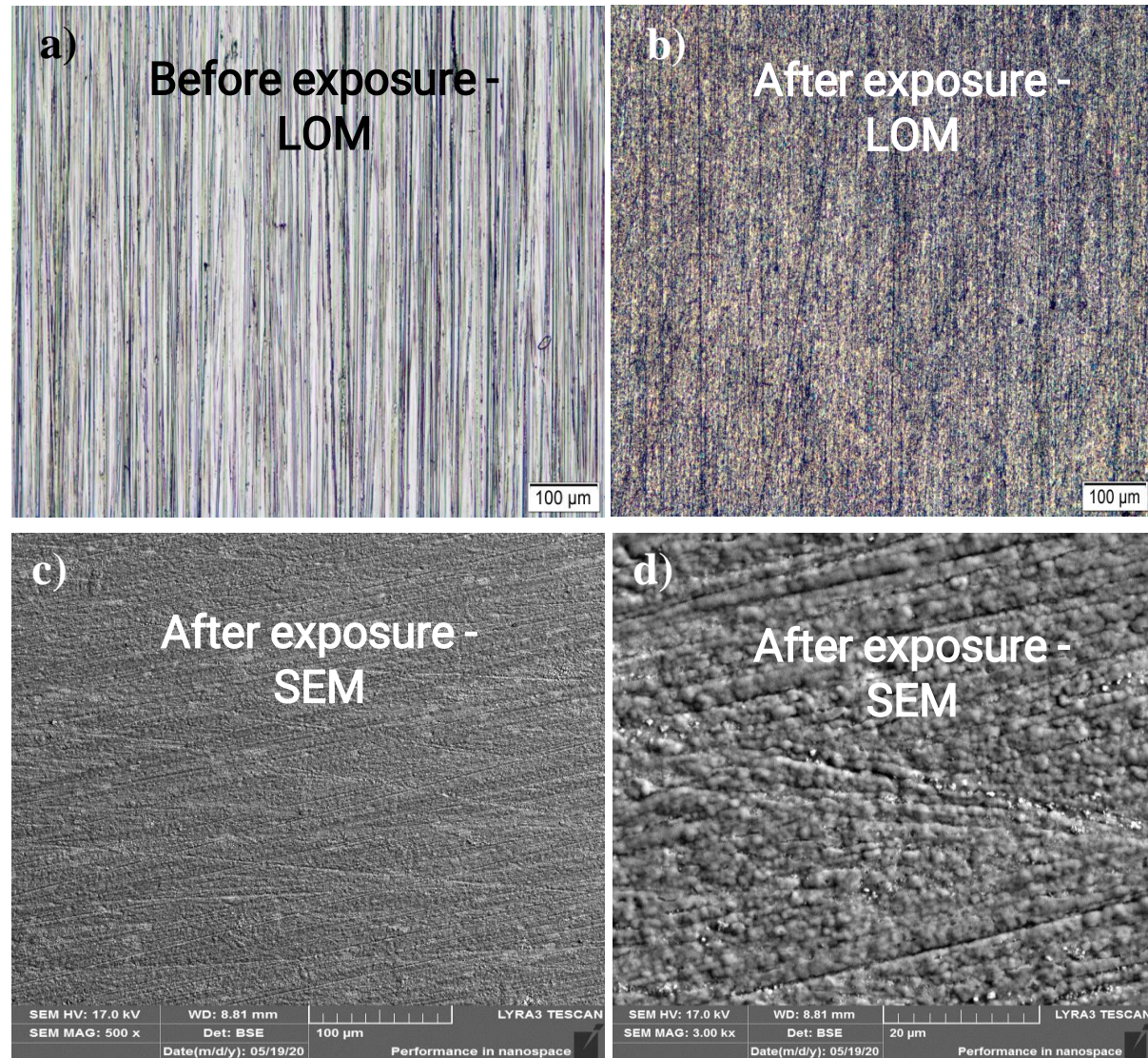


Figure: Surface morphologies of the 17-4-PH before (a) and after sCO2 exposure (b,c,d)

17-4-PH sample – cross section

- ❖ Optical surface analyses showed the different oxide thickness which means variability of colors
- ❖ This claim confirms cross section observation on the Fig
- ❖ Cross-section observation showed the formation of either a single Cr-O layer and also localized duplex spinel oxide
- ❖ Duplex spinel oxide is formed from outer Fe-O layer and inner Fe-Cr-O spinel
- ❖ Fe-Cr O spinel is formed inside to the steel

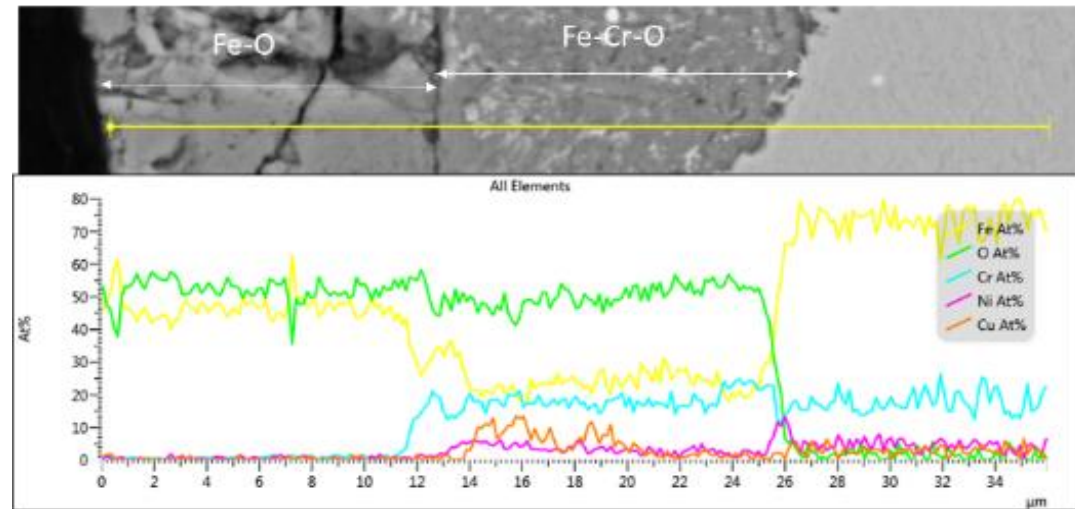
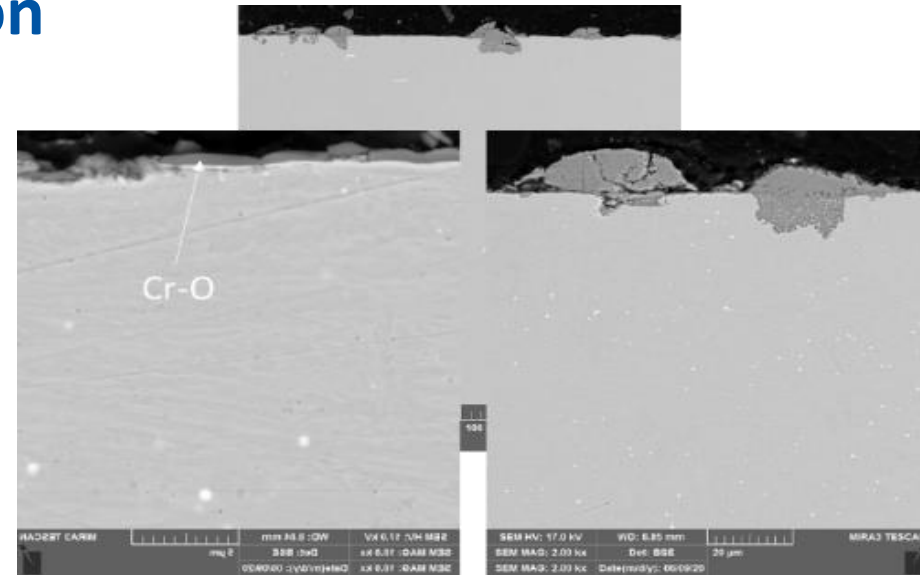


Figure: SEM cross section of the 17-4-PH and EDX linescan of the oxide layer

625M sample surface

- ❖ Fig. showed the surface morphology
- ❖ Many irregular, and discontinuous oxides were found on surface after exposure
- ❖ Different shades on the surface indicate different thicknesses and probably is possible the change in composition

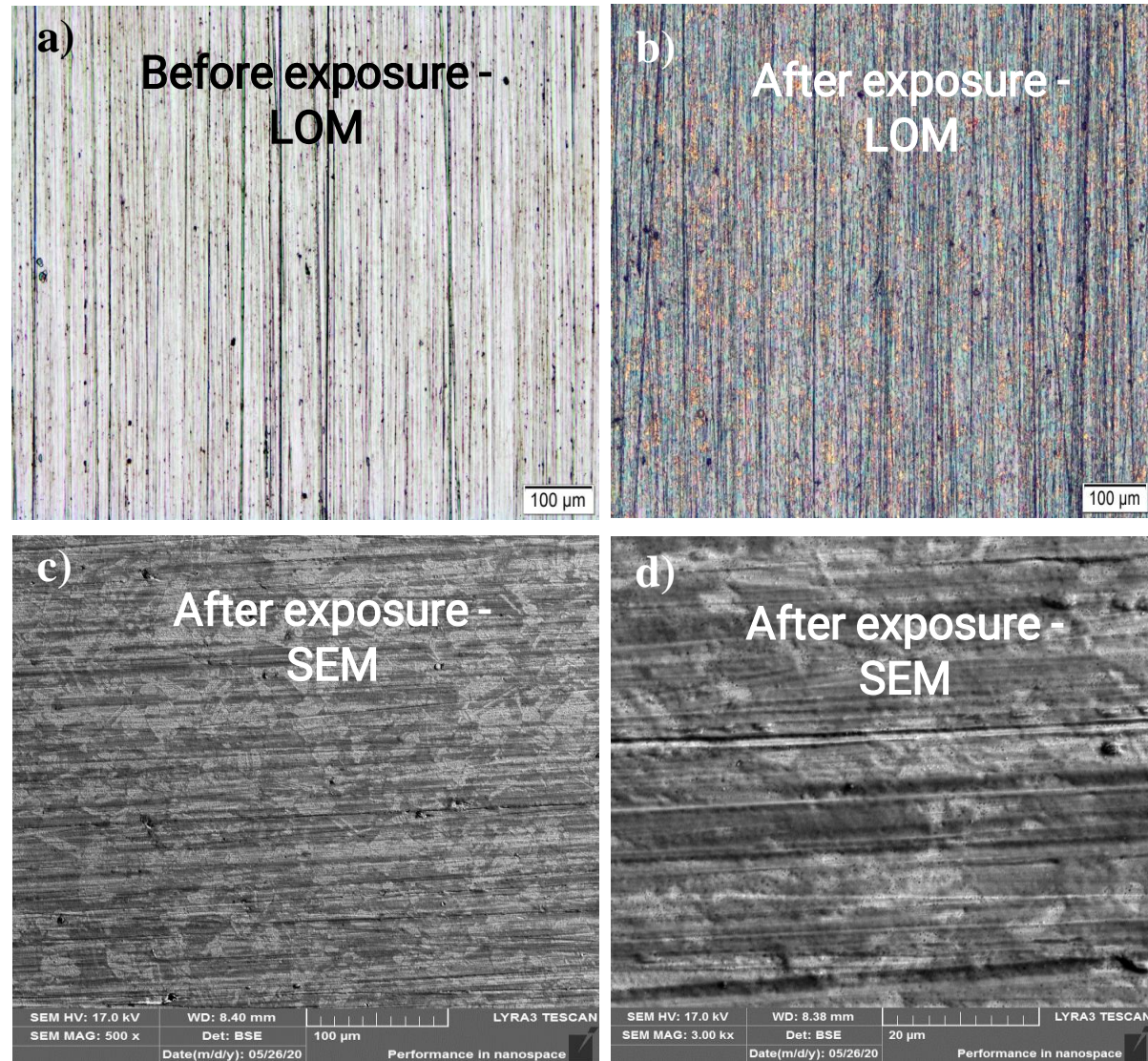


Figure: Surface morphologies of the 17-4-PH before (a) and after sCO2 exposure (b,c,d)

625M sample – cross section

- ❖ LOM and SEM of the surface observation suggested the different thickness of the oxide, which is confirmed by the analysis in cross-section
- ❖ EDS linescan of the oxide layer showed formation of two layers: outer layer of Cr-Ni-O, and an inner layer of Ni-Cr-O with depleted Cr part
- ❖ The oxide layer was not homogeneous
- ❖ XRD measurement showed that the main phase: iron nickel and chromium nickel
- ❖ Other phases: molybdenum nickel and chromium oxide

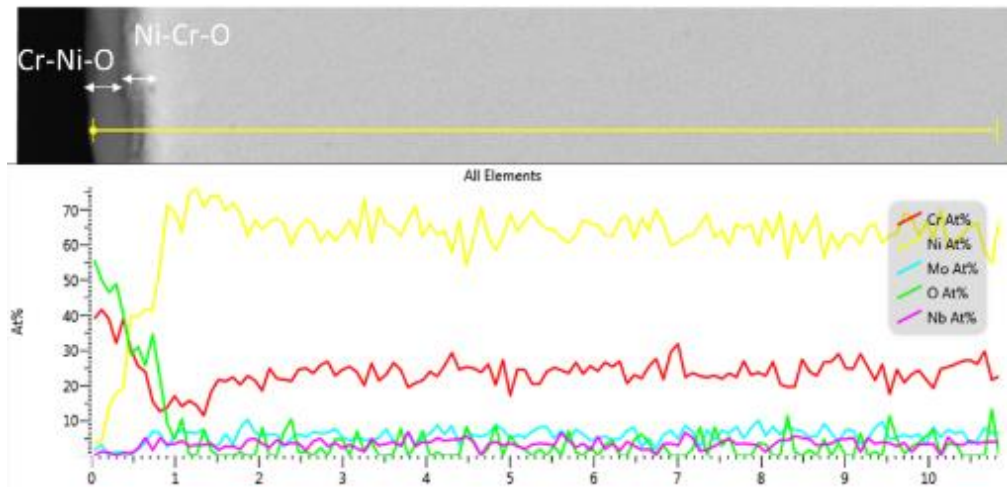
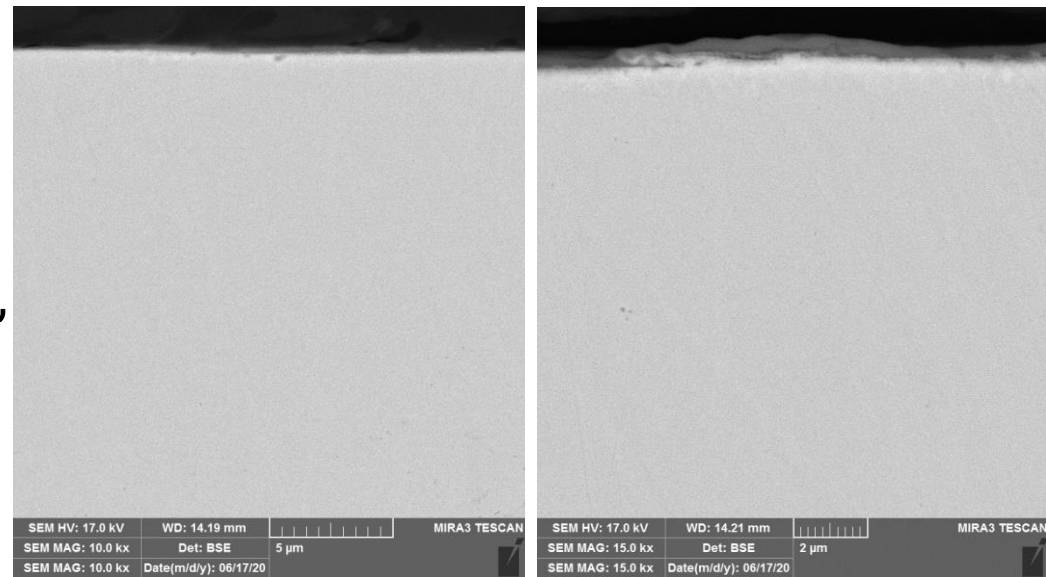


Figure: SEM cross section of the 625M and EDX linescan of the oxide layer

Inconel 718 sample - surface

- ❖ Fig. showed the surface morphology
- ❖ Many irregular, and discontinuous oxides were observed on Fig. b), c), d)
- ❖ Notably, numerous micrometer-sized nodular oxides were detected on Fig. d)

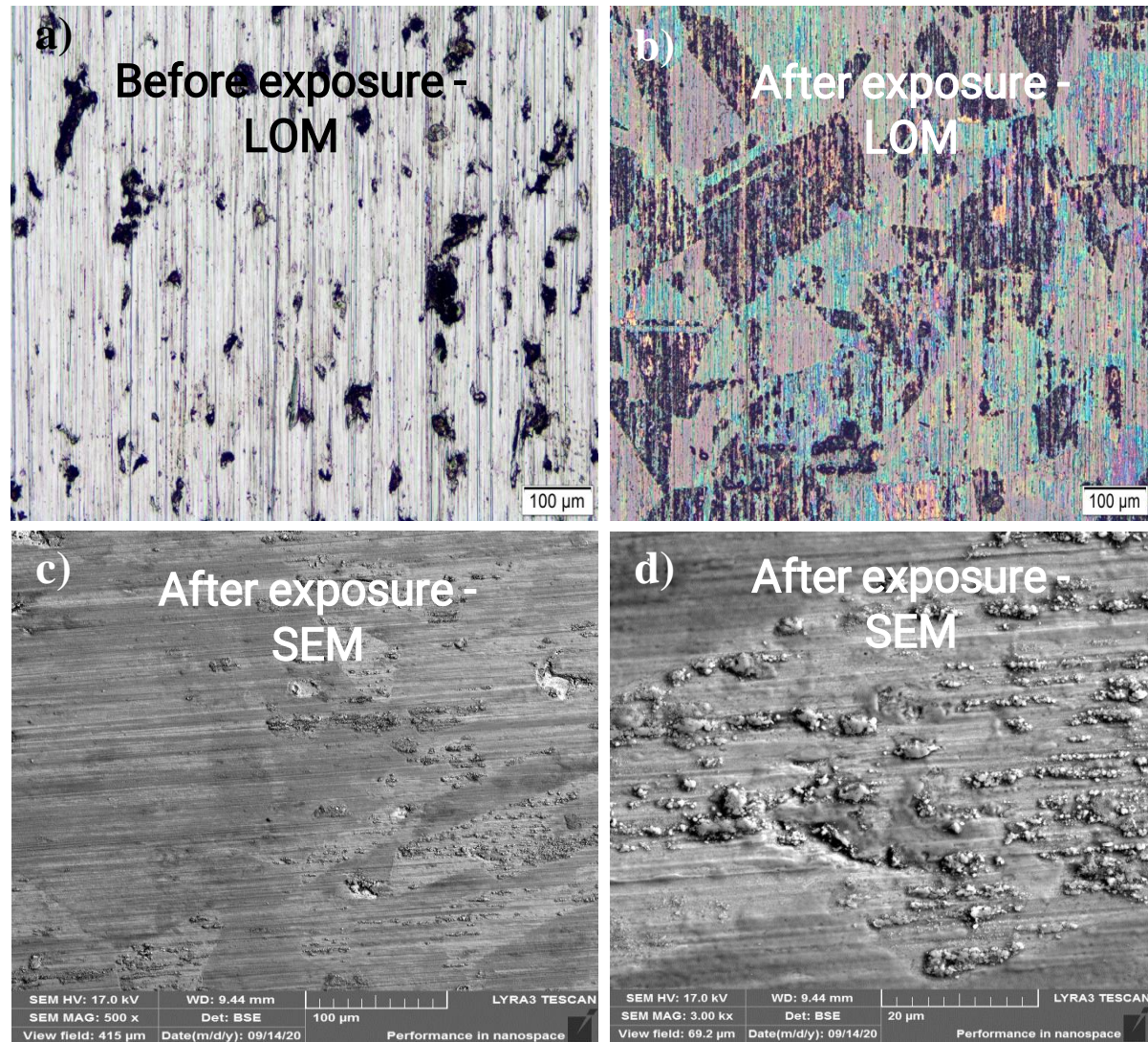


Figure: Surface morphologies of the In718 before (a) and after sCO2 exposure (b,c,d)

Inconel 718 sample – cross section

- ❖ LOM and SEM observation showed the uneven oxidation
- ❖ The Ni-base alloy In718 have a sufficient amount of Fe to develop an outer layer on the Fe-O
- ❖ Under the outer layer was observed the depleted part of Ni and Cr
- ❖ The cross-section also suggests the creation of the cracks or defects, probably
- ❖ XRD measurement showed the main phases: chromium nickel, chromium nickel
- ❖ Other phases: magnetite, niobium carbide

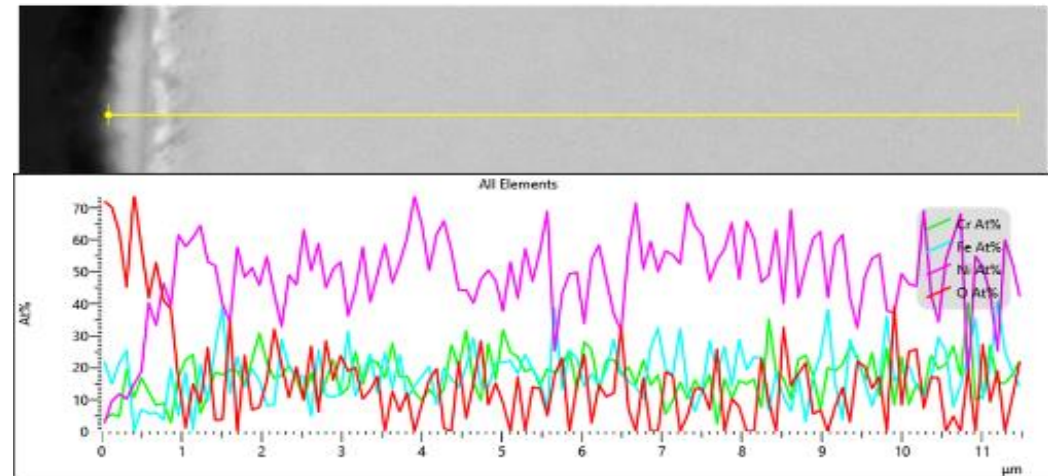
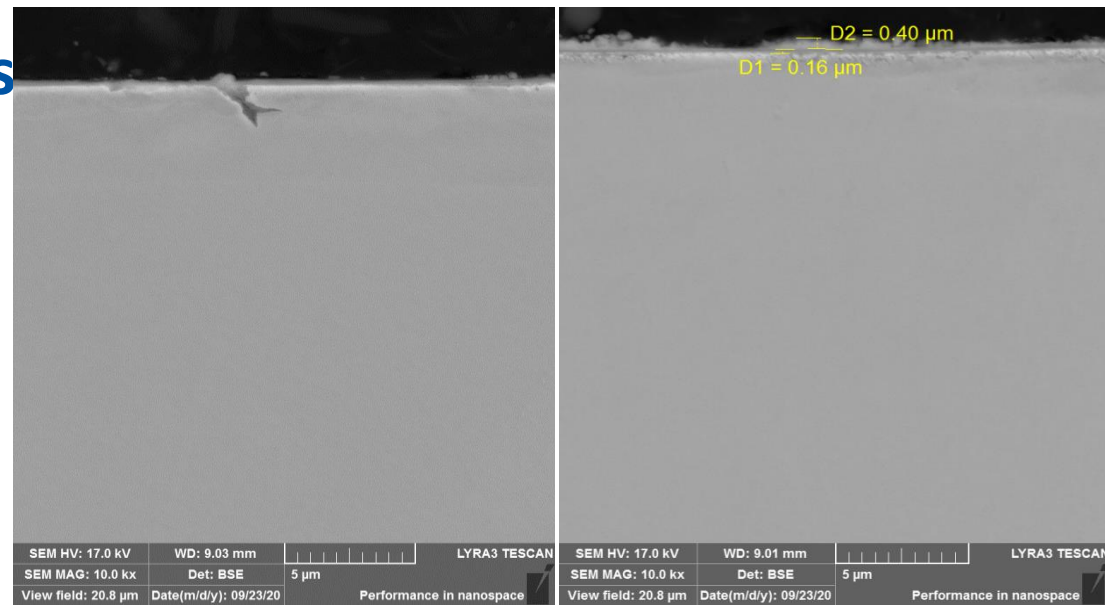
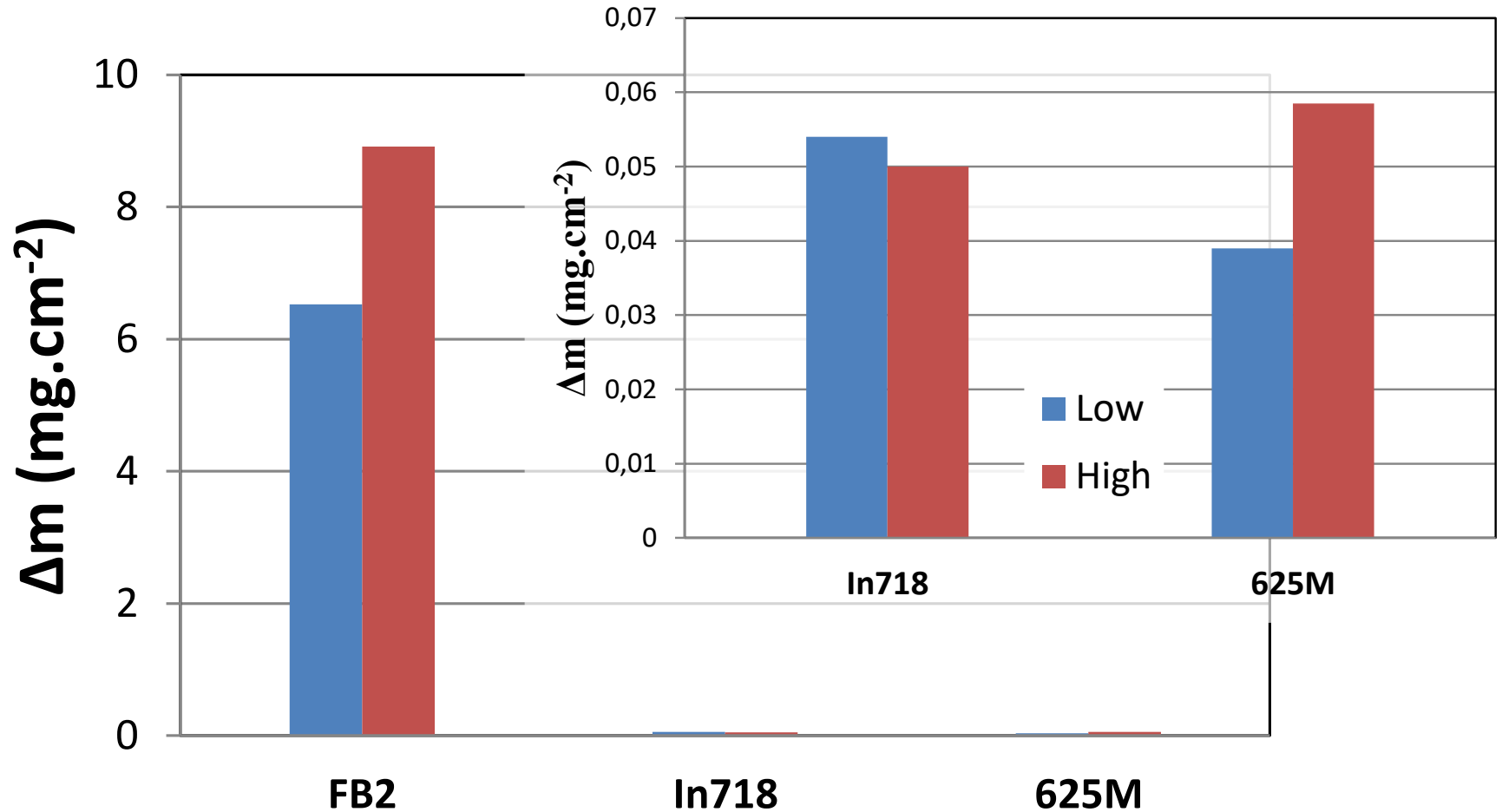


Figure: SEM cross section of the In718 and EDX linescan of the oxide layer

High-velocity flow effect

Average mass gain



High-velocity flow effect

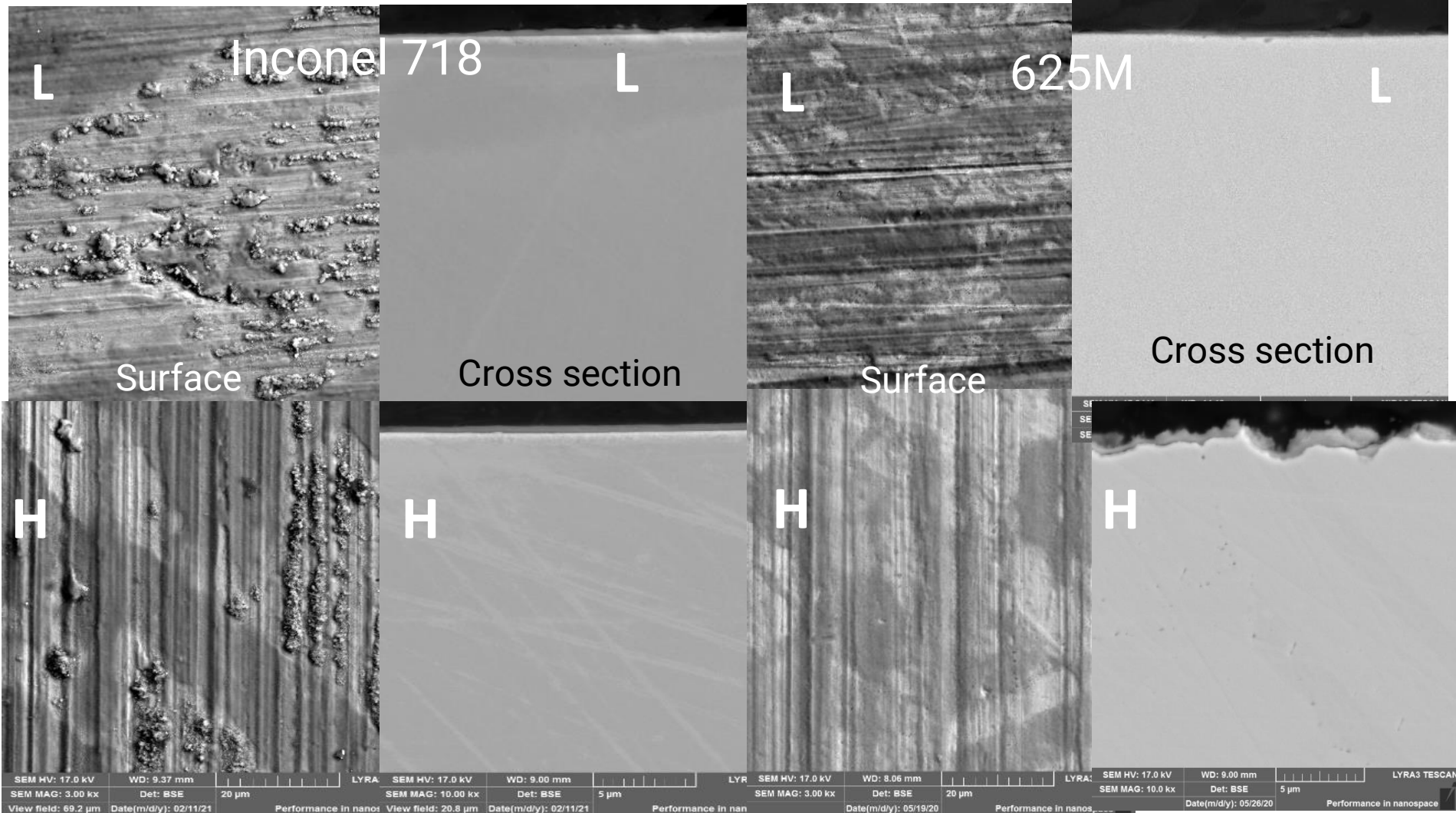


Figure: In718 (L) low-velocity, (H) high-velocity

Figure: 625M (L) low-velocity, (H) high-velocity

High-velocity flow effect

FB2

- ❖ Very high mass gain after the exposure (similar for both samples)
- ❖ Surfaces - homogenous layer
- ❖ EDX analyses - layers are formed by iron oxide
- ❖ Surface structure is rougher on the sample exposed to the lower velocity - evident slight erosion effect of the accelerated flow that makes the surface of the sample smoother
- ❖ Thickness of the oxidic layer is very similar for both samples

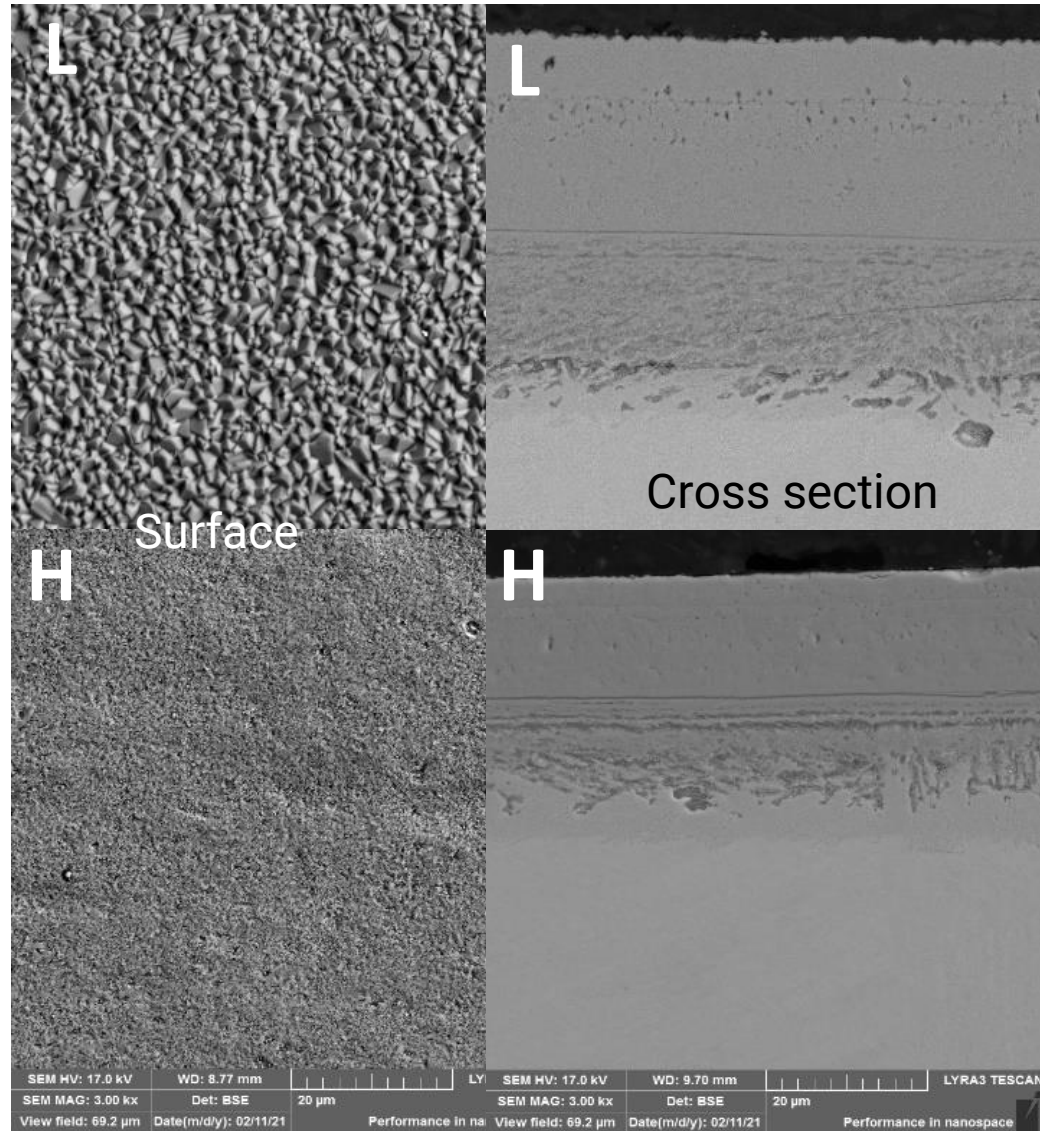


Figure: FB2 (L) low-velocity, (H) high-velocity

Conclusions

- ❖ The marked weight changes after exposure were observed on ferritic steel FB2 samples
- ❖ This weight changes correspond with thick and compact duplex oxide layer on the sample surface
- ❖ This layer may increase the thickness of outer layer with subsequent spalling during longer exposure in $s\text{CO}_2$ environment.
- ❖ The stainless steel 17-4-PH showed the different behavior. Marked nodules of the oxides on the surface and also under surface inside the material were observed.

Conclusions

- ❖ Chromia-forming alloys 625M and In718 showed better corrosion resistance than the FB2 and 17-4-PH due to the formation of the Fe-oxide or Cr-oxide rich scales on its surface. This result was mainly attributed to the higher Cr content in alloys 625M and In718. It was demonstrated that the corrosion performance of steels and alloys in supercritical carbon dioxide was mainly decided by the Cr content.
- ❖ 625M formed a dense and continuous Cr-O oxide layer with Ni content and exhibited an excellent corrosion resistance in high-temperature sCO₂ environment. The sufficient Cr in the interior of the alloy supports the stability of the Cr oxide layer.
- ❖ **The evaluation of corrosion test continues.**

The contact for questions

Lucia Rozumová

Researcher & research group leader



lucia.rozumova@cvrez.cz

Thank you for your attention

ACKNOWLEDGEMENTS

The presented work was financially supported by the H2020 sCO₂-FLEX project. This project has received funding from the European Union's Horizon 2020 research and innovation programme under grant agreement N^o 764690.

Some of presented results were obtained with support of Technology Agency of Czech Republic, project "Purification and purity control of CO₂ gas in power cycles" No. TK02030023.